Probability distributions and escape rates for systems driven by quasimonochromatic noise

M. I. Dykman

Department of Physics, Stanford University, Stanford, California 94305

R. Mannella

Dipartimento di Fisica, Universita di Pisa, Piazza Torricelli 2, 56100 Pisa, Italy

P. V. E. McClintock, N. D. Stein, and N. G. Stocks*

School of Physics and Materials, Lancaster University, Lancaster LA1 4YB, United Kingdom

(Received 19 November 1992)

The motion of an overdamped particle in a bistable potential $U(x)$, driven by quasimonochromatic noise (high-frequency, narrow-band noise), has been investigated by means of electronic analog simulation. The escape rate from one potential well to another was found to be exponentially small compared to the reciprocal mean first-passage time to the top of the potential barrier. The logarithm of the quasistationary probability distribution was observed to fall extremely sharply at a particular value of x, quite close to the equilibrium position. Theory describing the nonanalytic dependence of this logarithm on the bandwidth of the noise is presented and shown to be in good agreement with experiment. Data are also presented for a symmetric monostable potential. In a certain parameter range, the quasistationary distribution is demonstrated to be independent of the form of such a potential.

PACS number(s): 05.40.+j, 02.50.−r

I. INTRODUCTION

Fluctuations in physical systems can often be described by assuming that they are generated by external noise. Initial studies concentrated on the effect of Gaussian white noise, with correlator

$$\langle f(t)f(t')\rangle = D\delta(t - t'). \tag{1}$$

The white-noise approximation, which dates back to the work of Einstein [1] and Smoluchowski [2], is of course an idealization, not least because its power spectrum

$$\Phi(\omega) = \int_{-\infty}^{\infty} dt \exp(i\omega t)\langle f(t)f(0)\rangle \tag{2}$$

is flat and hence the total noise power is infinite for finite characteristic noise intensity D. For any real physical noise $f(t)$, the mean-square value $\langle f^2(t)\rangle$ is finite, and the power spectrum falls to zero as $|\omega| \to \infty$, i.e., $\Phi(\omega)$ is frequency dependent. Such noise is termed colored. For zero-mean stationary Gaussian noise, $\Phi(\omega)$ contains all information about the noise. Its form depends on the physical characteristics of the source of the noise itself and on the coupling between this source and the noise-driven system. For example, if the noise originates from coupling between the system and a heat bath, $\Phi(\omega)$ is determined by the density of states of the elementary excitations of the bath, by the temperature, and by the coupling constants. In many cases the noise power spectrum can be directly measured experimentally. It is therefore advantageous to express the characteristics of a fluctuating system in terms of $\Phi(\omega)$.

The effects of noise color have often been considered phenomenologically by assigning a given functional form to $\Phi(\omega)$. By far the most studied example is exponentially correlated noise [3], defined by

$$\langle f(t)f(t')\rangle = \frac{D}{2\tau} \exp(-|t - t'|/\tau),$$

$$\Phi(\omega) = D/(1 + \omega^2\tau^2). \tag{3}$$

In this case the noise is characterised by a single correlation time τ. White noise is recovered in the $\tau \to 0$ limit. (Note that some authors use the terms colored noise and exponentially correlated noise interchangeably.)

The quantity of primary interest in noise-driven systems is the probability-density distribution or distribution function. For weak noise this distribution is localized in the vicinity of the attractor(s) of the system. If the attractor is a stable state, the quasistationary distribution is, in general, Gaussian near the maximum. For many applications it is important, however, to find the distribution in regions far from the attractors. In contrast to the situation in the vicinity of a stable state, the distribution here is not of a universal form; it depends strongly both on the dynamics of the system in the absence of noise and on the *shape* of the noise power spectrum. First attempts at treating the exponentially correlated noise problem involved construction of approximate Fokker-Planck equations [3,4]. Unfortunately, solutions to such equations sometimes gave conflicting results. Subsequently, the problem was solved in the weak noise limit [5–10] using path-integral techniques [11] and the eikonal approxima-

tion to the exact multivariable Fokker-Planck equation [12–14].

In many physical situations the noise driving a system is more complicated. In particular, of great interest is "truly colored" noise, whose power spectrum peaks at a finite frequency ω_0, with the half width Γ satisfying

$$\Gamma \ll \omega_0. \tag{4}$$

An example of such noise is the electromagnetic field of incoherent, nearly monochromatic light. By analogy with optics and following [15] we shall call it *quasimonochromatic noise* (QMN).

QMN is generated by a variety of systems capable of singling out a frequency, and can be viewed as the result of filtering broadband noise through a highly selective system. Examples of such systems include various electromagnetic or acoustic high-Q cavities; their eigenvibrations excited at random by an external noise produce QMN [16,17]. Another familiar example is that of local and quasilocal (resonant) vibrations of impurities in crystals [18,19]. Such vibrations are mainly characterized by a single frequency and are coupled to a broadband of other modes of the crystal. Their thermal fluctuations are a typical QMN. The power spectra of local and resonant vibrations have been thoroughly investigated both theoretically and experimentally [18–22]. QMN can also be viewed as a narrow-band form of harmonic noise [23–25]. The latter has been invoked as a possible description of enzymatic catalysis.

The simplest type of QMN (which will be the specific form that we refer to as QMN below) is that produced by a harmonic oscillator of frequency ω_0 and damping Γ, driven by white noise

$$\ddot{f}(t) + 2\Gamma \dot{f}(t) + \omega_0^2 f(t) = \xi(t),$$

$$\langle \xi(t)\xi(t')\rangle = 4\Gamma T\delta(t - t'). \tag{5}$$

If the noise originates from coupling between the system and a heat bath, T may be identified as the temperature; more generally it is just a measure of the noise strength. The power spectrum of QMN has the form

$$\Phi(\omega) = \frac{4\Gamma T}{(\omega^2 - \omega_0^2)^2 + 4\Gamma^2\omega^2}. \tag{6}$$

In this paper we study the effect of QMN on simple physical systems and compare our observations with theoretical predictions. The previously published theory [26] describing the tails of the probability distribution of QMN driven systems worked to lowest order in the bandwidth Γ and reciprocal frequency ω_0^{-1}. Several unusual features were predicted, including square-root singularities and associated discontinuities in the logarithm of the probability distribution. Initial experimental investigations [15] demonstrated that this logarithm is continuous, although it varies very steeply in the range where theory predicted a discontinuity. A higher-order perturbation theory and a fuller set of experimental data are given in the present paper.

Section II provides a qualitative explanation of the features of the original theory. Experimental results, obtained by electronic analog simulation of a particle in a bistable potential, and also by digital-computer simulation, are presented in Sec. III. The main result is that a particle initially in one potential well can cross the potential barrier top (PBT) several times, back and forth, but still return to the initially occupied well with overwhelming probability, instead of making a transition to the other well. This is in sharp contrast to the situation for simple dynamical systems driven by both white and exponentially correlated noise, where a fluctuation driving the particle just over the PBT is sufficient to cause a transition [6,8,27]. Section IV substantially extends the theory to account for the smearing out of the discontinuities in the logarithm of the probability density evident in the experimental data. The smearing is found to depend nonanalytically on Γ. Section V discusses the features of QMN-induced fluctuations in monostable systems and Sec. VI contains concluding remarks. The Appendix presents a numerical algorithm for Monte Carlo simulation of a QMN-driven system.

II. QUASISTATIONARY PROBABILITY DISTRIBUTION IN THE ADIABATIC APPROXIMATION: INTUITIVE RESULTS

The dynamics of a system driven by colored noise is characterized by the noise correlation time (times) τ as well as the relaxation time (times) t_r in the absence of noise. If the system is bi- or multistable, other important characteristic times are the reciprocal probabilities W_{ij}^{-1} of noise-induced transitions between the stable states i, j. For sufficiently weak noise the transition probabilities are small

$$W_{ij}t_r \ll 1, \qquad W_{ij}\tau \ll 1. \tag{7}$$

[In fact, the conditions (7) are necessary for the concept of transition probability to be meaningful; the transition probability would otherwise depend on the initial position of the system and/or the initial state of the noise, and one would arrive at a continuum of "transition probabilities" when considering a distribution of initial states.] If (7) are fulfilled and a system is placed initially in the range of attraction to a stable state i, then in the time range

$$t_r, \tau \ll t \ll W_{ij}^{-1} \tag{8}$$

the probability distribution p_i over the phase space of the system in the vicinity of the state i is virtually time independent. (We note that finding the boundary of the range of quasistationarity is a nontrivial problem. In particular, as was shown in [15,26], this boundary depends on the shape of the power spectrum of the noise.)

This paper examines the effect of QMN on an overdamped particle in a potential $U(x)$. The motion of the particle is described by the Langevin equation

$$\dot{x} + U'(x) = f(t). \tag{9}$$

We consider the situation where time scales are widely

separated

$$\Gamma \ll t_r^{-1} \ll \omega_0. \tag{10}$$

Here the relaxation time $t_r = \max\{[U''(x_i)]^{-1}\}$, where x_i are the minima of $U(x)$. In this section we give a simple qualitative derivation of the quasistationary probability density in the adiabatic approximation. The full calculation, which has the advantage that it can be extended to include nonadiabatic corrections, but which requires use of path-integral theory, is deferred to Sec. IV.

We note first of all that QMN as given by Eq. (5) can be viewed as vibrations at frequency ω_0 with random amplitude and phase. To describe these vibrations it is convenient to change from $f(t), \dot{f}(t)$ to new variables $f_{\pm}(t)$

$$f(t) = \sum_{\alpha=\pm} f_\alpha(t) \exp(i\alpha\omega_0 t),$$

$$\dot{f}(t) = \sum_{\alpha=\pm} i\alpha\omega_0 f_\alpha(t) \exp(i\alpha\omega_0 t). \tag{11}$$

We emphasize that no approximations have been made at this stage; Eq. (11) is just a definition of $f_{\pm}$ in terms of f and $\dot{f}$. It is clear from (5) that the amplitudes $f_{\pm}(t)$ depend on time comparatively smoothly

$$\langle |\dot{f}_{\pm}(t)|^2 \rangle \sim \Gamma^2 \langle |f_{\pm}(t)|^2 \rangle. \tag{12}$$

The stationary probability distribution $p(\mathrm{Re} f_+, \mathrm{Im} f_+)$ of the variables $f_{\pm}(t)$ can readily be obtained, since Eq. (5) allows $f(t)$ and $\dot{f}(t)$ to be associated with the position and velocity of a harmonic oscillator coupled to a thermal bath of temperature T. The probability distribution is therefore of Boltzmann form; its dependence on f and $\dot{f}$ is solely through the energy E

$$p(E) \propto \exp(-E/T).$$

Since, in view of (11), $E = \frac{1}{2}\dot{f}^2 + \frac{1}{2}\omega_0^2 f^2 = 2\omega_0^2 |f_+|^2$,

$$p(\mathrm{Re} f_+, \mathrm{Im} f_+) = \frac{2\omega_0^2}{\pi T} \exp(-2\omega_0^2 |f_+^2|/T). \tag{13}$$

In response to the nearly periodic forcing, the coordinate $x(t)$ oscillates at the same frequency ω_0, with smoothly varying amplitude and phase. However, because in general the potential is nonlinear and asymmetric about the stable point in the absence of forcing, not only do the amplitude and phase change, but the center of vibration also moves. To describe this effect we write

$$x(t) = \sum_{\alpha=\pm} x_\alpha(t) \exp(i\alpha\omega_0 t) + x_c(t). \tag{14}$$

Substituting (14) into (9) and allowing for the fact that, on the one hand, the frequency ω_0 is much higher than the relaxation rate of the system and, on the other hand, the latter greatly exceeds the rate at which the amplitudes $f_{\pm}$ change, we get

$$x_\alpha(t) \simeq f_\alpha(t)/(i\alpha\omega_0), \qquad \alpha = \pm. \tag{15}$$

Although higher harmonics can formally be included in $x_\alpha(t)$ and $x_c(t)$ in (15), they are small and will be neglected. [The nth harmonic is of order $|U^{(n+1)} x_+^n|/n\omega_0 \ll |x_+|$ for small $(\omega_0 t_r)^{-1}$.]

To find the smooth function x_c it is convenient to introduce an auxiliary three-variable potential, by averaging $U(x)$ over the period of oscillation

$$V(x_c, x_+, x_-) = \frac{1}{2\pi} \int_0^{2\pi} d\psi \, U(x_c + x_+ e^{i\psi} + x_- e^{-i\psi}), \tag{16}$$

$$\psi = \omega_0 t.$$

Averaging (9) and working to lowest order in $(\omega_0 t_r)^{-1}$ gives

$$\dot{x}_c = -V_c'(x_c, x_+, x_-), \qquad V_c' \equiv \frac{\partial V}{\partial x_c}. \tag{17}$$

Equations (12) and (15) show that the complex amplitudes $f_{\pm}(t)$ and hence $x_{\pm}(t)$ vary over a time $\sim \Gamma^{-1}$, which greatly exceeds the characteristic relaxation time t_r of x_c. Therefore x_c follows the variation of $x_{\pm}(t)$ adiabatically, and the $\dot{x}_c$ term in (17) may be neglected, yielding

$$V_c'(x_c^{(\mathrm{ad})}, x_+, x_-) = 0, \tag{18}$$

which determines x_c implicitly

$$x_c(t) \simeq x_c^{(\mathrm{ad})}(x_+, x_-). \tag{19}$$

In other words, the center of vibrations sits at the minimum of the smoothed potential V as shown in Fig. 1.

It is now possible to find the logarithm of the probability distribution $p_i(x)$ of the system far from the equilib-
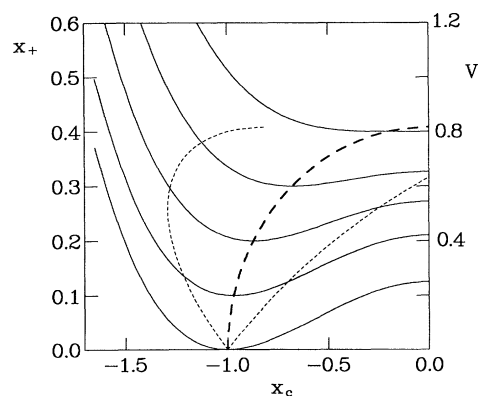

FIG. 1. The smoothed potential $V(x_c)$ (solid lines) resulting from the particular case $U(x) = -\frac{1}{2}x^2 + \frac{1}{4}x^4$, for various values of the oscillation amplitude x_+. The lowest curve is for $x_+ = 0$; each subsequent curve increments the value of x_+ by 0.1. The heavy dashed line shows the evolution of x_c (plotted horizontally) as a function of x_+. The extreme limits of oscillation $x_c - 2x_+$, $x_c + 2x_+$ are also shown (light dashed lines). Note that the left limit does not go beyond $-\sqrt{5/3} \simeq -1.29$.

rium position x_i. The distribution in this range is formed by occasional, comparatively large outbursts of the noise $f(t)$. We need to express the probability of the appropriate outburst as given by (13) in terms of x. It suffices to express the position x in terms of x_+, since $p_i(x)$ can then be obtained (up to a prefactor) by using (15) to replace f_+ by x_+ in (13). The time origin is chosen so that the point x is reached at $t = 0$

$$x = x_c(0) + x_+(0) + x_-(0). \qquad (20)$$

By far the most probable way of reaching x, is if the particle arrives there just when the fluctuations reach their maximum amplitude. The condition for this is

$$x_+(0) = x_-(0). \qquad (21)$$

Equations (19)–(21) give the required relation between x and x_+. According to (13) the expression for the probability density is

$$\ln[p_i(x)/p_i(x_i)] = -R_i(x)/D \qquad [R_i(x) \gg D] \quad (22)$$

where

$$R_i(x) = \frac{2\omega_0^2}{\Gamma}|x_+(0)|^2. \qquad (23)$$

Here D is a rescaled noise intensity, equal to the maximum value of the power spectrum of the noise

$$D = \Phi_{\max}(\omega) = T/\Gamma\omega_0^2. \qquad (24)$$

The dependence of the probability distribution $p_i(x)$ on D is thus of the activation type, and $R_i(x)$ may be called an activation energy for reaching the point x by the system in the ith stable state.

We stress that Eqs. (22)–(24) have been derived in the double-adiabatic approximation. On one hand, the central frequency ω_0 of the power spectrum of the noise was assumed to exceed substantially the relaxation rate of the system and, on the other hand, the latter was assumed to exceed the bandwidth of the noise.

Two specific consequences follow immediately from Eqs. (18)–(21) and (23) [26]. The first applies to a monostable, symmetric potential where $U(x) = U(-x)$. (We have chosen the origin to coincide with the equilibrium position.) In this case, $V(x)$ has only one minimum, at $x = 0$, so that $x_c^{(ad)} = 0$ and $x_\pm(0) = \frac{1}{2}x$, with the activation energy

$$R_i(x) = \frac{\omega_0^2}{2\Gamma}x^2. \qquad (25)$$

The distribution given by (22) and (25) is of the form of that for a system with a *parabolic* potential [although $U(x)$ is *not* parabolic, in general] but, remarkably, its shape is independent of $U(x)$.

The other feature can arise for a potential asymmetric about the minimum. It is related to the fact that as the noise amplitude $\propto |f_+(t)|$ increases, not only does the amplitude of oscillations in $x(t)$ increase in proportion to $|f_+(t)|$, but also their center is shifted. If this

shift is comparatively strong, then as $|f_+(t)|$ and $|x_+(t)|$ vary, the extreme value attained by $x(t)$ will not enter the range beyond the limiting value $\bar{x}$ given by (20), (21), and the equation

$$\left.\frac{dx}{dx_+(0)}\right|_{x=\bar{x}} = 0, \qquad x_\pm(0) = \bar{x}_\pm. \qquad (26)$$

This behavior is clearly seen in Fig. 1. The range of x encountered in the forced vibrations does not spread beyond a certain point. Taking into account the interrelation (19) between $x_c^{(ad)}$ and $x_\pm$, one can rewrite Eq. (26) as

$$V_{cc}'' = V_{c+}'' \quad \text{for} \quad x_\pm = \bar{x}_+ = \bar{x}_-, \qquad x_c = x_c^{(ad)}(\bar{x}_+, \bar{x}_-) \qquad (27)$$

$$V_\alpha' = \frac{\partial V}{\partial x_{-\alpha}}, \qquad V \equiv V(x_c, x_+, x_-)$$

(Subscripts α, c denote derivatives with respect to $x_{-\alpha}, x_c$ respectively. The number of primes indicates the total order of the derivative.)

It is obvious from (26) that for x close to $\bar{x}$ the difference $x_+(0) - \bar{x}_+$ varies as $[C(x - \bar{x})]^{\frac{1}{2}}$. (The constant C can easily be expressed in terms of the derivatives of V; see below.) Therefore

$$R_i(x) = R_i(\bar{x}) - [C'(x - \bar{x})]^{1/2}, \qquad C' = \text{const}, \qquad (28)$$

i.e., the effective activation energy for reaching a point x has a square-root singularity and is discontinuous at $x = \bar{x}$. We stress that this singularity can arise even if the potential $U(x)$ of the system itself is perfectly smooth; it is not associated with any singular points of $U(x)$, although the onset of the singularity depends solely on the form of $U(x)$ and is independent of the parameters of the noise.

III. ANALOG EXPERIMENTS

A. Experimental details

Quasistationary distributions and escape rates were measured using electronic analog simulation, in which the variables x and f are represented by voltages in an electronic circuit [28]. A harmonic-oscillator circuit was driven by noise from a feedback shift-register noise generator [Fig. 2(a)]. The integrators in the circuit had a time constant $\tau_I = 1$ ms. As this is orders of magnitude greater than the noise correlation time, $\tau_N = 4.53$ μs, the noise was perceived as white, with characteristic intensity

$$T = \frac{1}{2\Gamma}\frac{\langle V_N^2\rangle\tau_N}{\tau_I}, \qquad (29)$$

where V_N is the noise voltage. The output from this circuit is just QMN and was used to drive a second circuit modeling Eq. (9) [Fig. 2(b)] for the symmetric, bistable
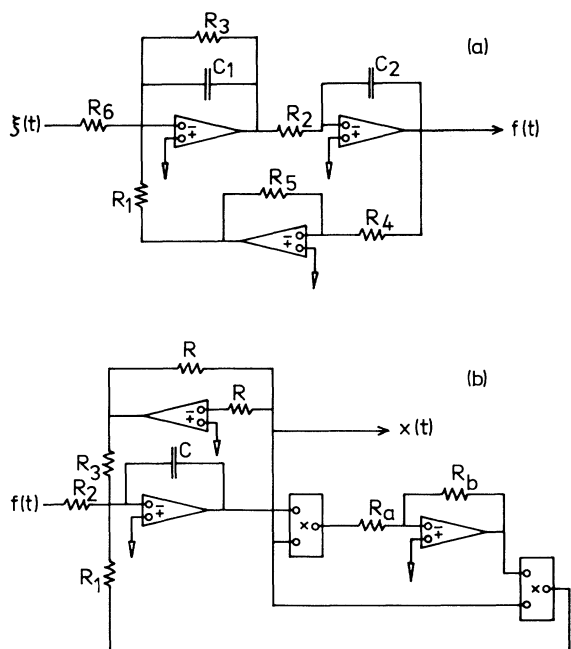
FIG. 2. Block diagrams of the electronic circuits used in the simulation. (a) Circuit used to convert white noise into QMN. (b) Circuit modeling an overdamped particle in the potential $U(x) = -\frac{1}{2}x^2 + \frac{1}{4}x^4$.

potential

$$U(x) = -\frac{1}{2}x^2 + \frac{1}{4}x^4 \tag{30}$$

for which minima occur at $x_1 = -1$ and $x_2 = +1$ with a maximum at $x = 0$.

The QMN parameters are nominally determined by the resistances R_1–R_3:

$$\omega_0^2 = R_2/R_1, \qquad 2\Gamma = R_2/R_3. \tag{31}$$

When compared with measured values, the second expression was found to break down for $\Gamma \leq 0.1$. It is not known why this should be the case. The damping was measured in two different ways. First, it is well known that the probability density for a system driven by white noise obeys the Maxwell distribution over velocities [27]

$$P(\dot{f}) \propto \exp(-\dot{f}^2/2T)$$

from which it follows that $\langle \dot{f}^2 \rangle = T$. On measuring $\langle \dot{f}^2 \rangle$ and $\langle V_N^2 \rangle$, the value of Γ follows from (29). The alternative method was to switch off the white noise, and instead drive the oscillator by a sine wave of amplitude A, whose frequency was adjusted until resonance was achieved. One can then find Γ and ω_0 from the amplitudes of $f(t)$ and $\dot{f}(t)$ which are equal to $A/(2\Gamma\omega_0)$ and $A/(2\Gamma)$, respectively. The two methods agreed to within 5%.

The output voltage x was digitized by a Nicolet 1080 data processor into blocks of 4096 samples. After ini-

tial processing, the data could later be transferred to a mainframe computer for further analysis.

B. Escape rates

One of the most important problems in multistable noise-driven systems is to determine the rate at which particles escape from one well to another. In the white-noise case, a system that has just crossed the potential barrier top changes wells with a probability of order $\frac{1}{2}$. However, the problem is quite nontrivial in the present case of QMN, as exemplified by Fig. 3(a), which shows typical time series $x(t)$, one for each well. Motion on two
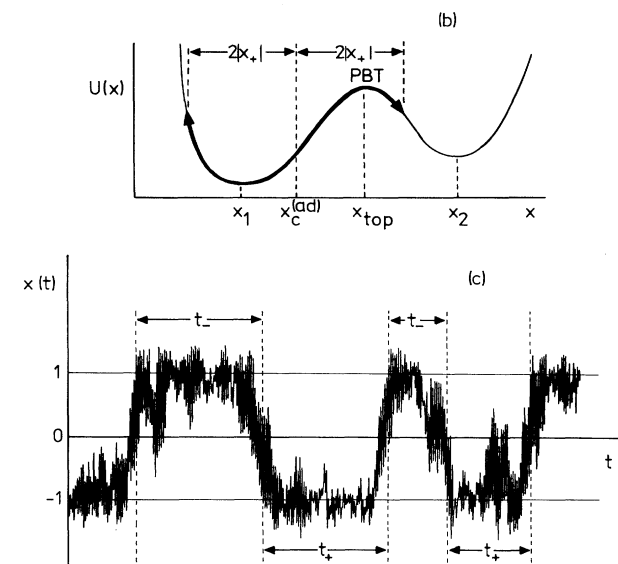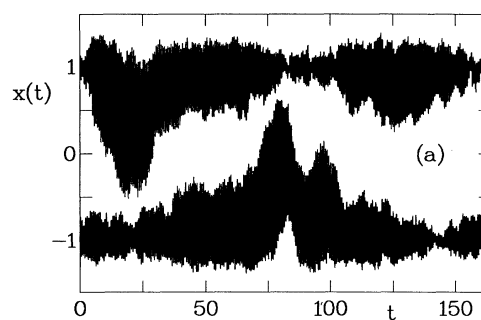

FIG. 3. (a) Two time series $x(t)$, one for each potential well, measured with $\Gamma = 0.021$, $\omega_0 = 9.81$, $D = 192$. Although the particle frequently crosses $x = 0$, the oscillations are not (quite) large enough to cause a transition. (b) Schematic illustration of the motion in (a). The coordinate oscillates (thick line with arrows) with amplitude $2|x_+|$ about a center of motion $x_c^{(ad)}$, and can pass PBT on each cycle without making a transition out of the initially occupied potential well. (c) The program determines the times t_+, t_- separating first crossings of the two criterion levels, here set equal to ± 1. Two separate distributions are created, for upwards and downwards transitions, respectively, by acquiring and analyzing a large number of $x(t)$ blocks and averaging the results.

different time scales is evident: rapid oscillations of frequency ω_0 are accompanied by a slow drift of the center of oscillations x_c. Equation (15) states that the amplitude of the oscillations $|x_+|$ is proportional to the size of the noise fluctuations. An outburst of sufficiently large fluctuations will cause oscillations so large that the particle will cross and recross the potential barrier several times. Nevertheless, an interwell transition does not occur because x_c still lies in the original well, and when the fluctuational outburst decays the system returns to the stable state occupied initially. The situation is illustrated schematically in Fig. 3(b) for a general (asymmetric) potential. As the size of the driving fluctuations increases still further, x_c approaches x_{top}, the position of the PBT and eventually crosses it. [The explicit relationship between x_+ and x_c is given by Eq. (19).] Only then does a transition between wells take place. This is one of the most remarkable features of QMN [15,26]. The mean time to escape from one potential well to the other was obtained by setting two reference levels, typically $x = \pm 1$, measuring the distribution of passage times between the levels, and averaging. The results turned out to be insensitive to changes of the reference levels within reasonable limits. The data processor divides the time series $x(t)$ into discrete blocks of duration

$$t_{\text{max}} = (\text{block size}) \times (\text{dwell time}),$$

where the block size is the number of points per block (in this case 4096) and the dwell time is the time interval between samples. Each block is analyzed independently. It should be noted that any transition straddling more than one block will be missed and that this may give rise to a distortion of the resultant distribution. Two different algorithms were used for analysis of the $x(t)$ data. In each of them, the program measured the time interval separating each pair of successive level crossings [see Fig.

3(c)], and then incremented the corresponding points in the memory blocks in which the passage-time distributions were being formed: separate blocks were used for the distributions of upwards and downwards level crossings. In the first algorithm, the maximum time of the distributions was equal to t_{max}. This meant not only that passage times longer than t_{max} would inevitably be missed, but also that shorter passage times than t_{max} would effectively be underweighted because the initial level crossing would not, in general, be at the start of the $x(t)$ block. In the second algorithm, this problem was avoided by making the maximum time in the distribution equal to $t_{\text{max}}/4$ and terminating new passage-time searches $t_{\text{max}}/4$ *before* the end of the $x(t)$ block. Thus all passage times less than $t_{\text{max}}/4$ would have had an equal chance of being observed, regardless of the time at which the initial level crossing occurred in $0 < t < 3t_{\text{max}}/4$. Distributions measured in this way exhibited a sharp cutoff at $t_{\text{max}}/4$.

The distortion in the distributions determined with the first algorithm could be corrected in two ways. One can assume the time distribution of escape times is exponential, with mean escape time T. This is reasonable because escapes are rare and therefore uncorrelated. The observed distribution is then

$$p(t) = N \left(1 - \frac{t}{t_{\text{max}}} \right) \exp(-t/T), \quad t < t_{\text{max}}$$

$$p(t) = 0, \qquad t > t_{\text{max}}. \tag{32}$$

(N is a normalization factor.) Averaging gives a relationship between the observed mean escape time and T. Alternatively, to a good approximation, exactly one transition per block is missed provided t_{max} is several times larger than T. The mean escape time is given by

$$T = \frac{(\text{total time of observation})}{(\text{number of transitions observed}) + (\text{number of blocks})}. \tag{33}$$

The corrected escape times for the two methods were in agreement over a wide range of dwell times.

Theory [26] predicts that the mean escape time varies exponentially with inverse noise strength:

$$T \propto \exp(R_{it}/D), \tag{34}$$

where $R_{it} = \frac{1}{3}\omega_0^2/\Gamma$ for the potential under consideration. Mean escape times obtained by analog simulation are shown in Fig. 4. When plotted in the form $\ln T$ versus $1/D$ the data lie on a straight line to an excellent approximation. Its slope, $R_{it} = 1600$ for $\omega_0 = 9.81$, $\Gamma = 0.021$; and $R_{it} = 719$ for $\omega_0 = 9.95$, $\Gamma = 0.045$. These values are gratifyingly close to the theoretical predictions of 1528 and 733, respectively.

Comparison with Fig. 5, derived from measurements of quasistationary distributions (see below), shows that R_{it} is substantially greater than the activation energy required to reach the potential barrier top R_i (0) = 910

($\Gamma = 0.021$), R_i (0) = 467 ($\Gamma = 0.045$). For the lowest D investigated with $\Gamma = 0.021$, R_{it}/D and R_i (0)/D were equal to 12.1 and 6.89, respectively, confirming that the probability of reaching the PBT exceeded the transition probability by a factor of approximately 100.

As a further check, digital simulations were performed using a Monte Carlo technique discussed in the Appendix. Figure 4 shows them to be fully consistent with the analog experiments, and hence also with theory.

C. Quasistationary distributions

On time scales short compared to W^{-1}, the center of oscillations is confined to one potential well with overwhelming probability and the position of the particle is described by a quasistationary distribution. Experimental quasistationary distributions obtained for the left-hand well are plotted in Fig. 5.
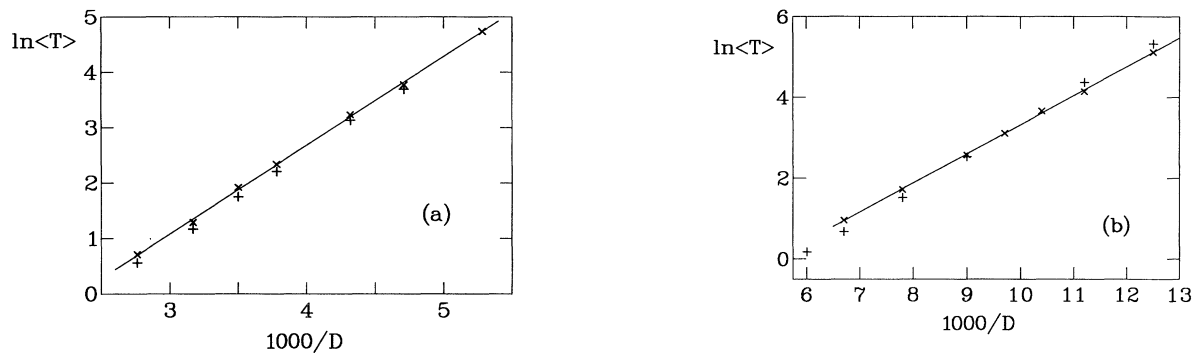
FIG. 4. Mean escape times as a function of the inverse noise strength. Crosses and pluses represent analog and digital simulation, respectively (a) $\omega_0 = 9.81$, $\Gamma = 0.021$, (b) $\omega_0 = 9.95$, $\Gamma = 0.045$. The straight line is a fit to the analog data.
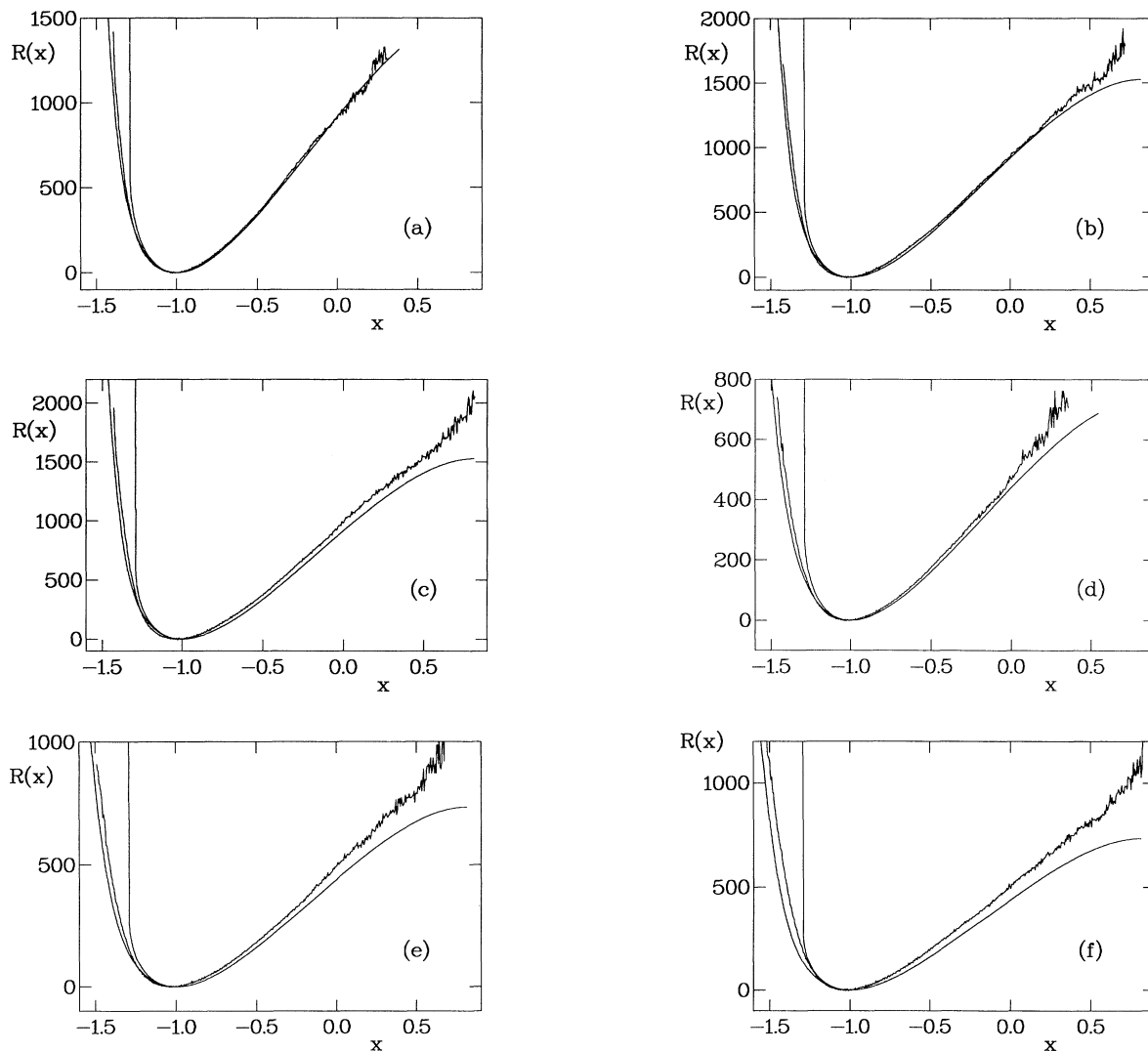

FIG. 5. Quasistationary distributions centered on $x = -1$, plotted in activation energy form $R = D|\ln[p(x)/p(-1)]|$. In (a)–(c) $\omega_0 = 9.81$, $\Gamma = 0.021$ and the noise intensity is (a) $D = 132$, (b) $D = 189$, (c) $D = 231$. In (d)–(f) $\omega_0 = 9.95$, Γ = 0.045, with noise intensities (d) $D = 80$, (e) $D = 111$, (f) $D = 150$. The jagged line (i.e., the central line for $x < -1$) is experimental data, the smooth line which becomes vertical at $x \simeq -1.29$ is adiabatic theory and the leftmost smooth line (plotted for $x < -1$) is theory corrected for nonadiabatic effects.
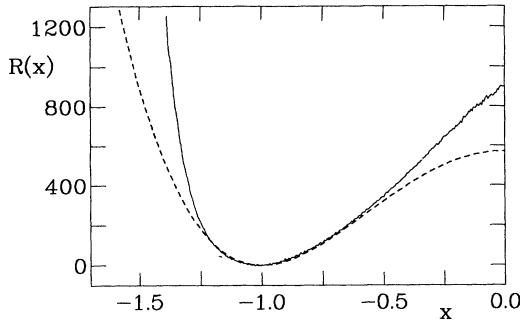
FIG. 6. Comparison of quasistationary distributions for white noise and QMN with $\Gamma = 0.021$, $\omega_0 = 9.81$. Solid line is QMN (experiment) with $D = 132$. Dashed line is white noise (theory) with D chosen so that the two curves have same curvature at $x = -1$.

For the weakest noise intensities considered, no inter-well transitions occurred during the period of observation and data acquisition was therefore straightforward. For stronger noise occasional transitions were, however, encountered. This problem was overcome by rejecting any block of data in which the $x(t)$ signal exceeded a certain level, typically 0.9. We emphasize that complete blocks were rejected, not just those points satisfying $x >$ 0.9. Thus the distributions obtained were not contaminated by $x(t)$ trajectories leading up to or from a transition. That the distributions obtained were insensitive to the exact choice of cutoff level gives extra confidence that this procedure is equivalent to observing over much shorter time intervals (in which no transitions occur) and averaging the results in order to reduce random scatter to an acceptable level.

The data agree very well with the adiabatic theory outlined in Sec. II when $x \geq \bar{x} = -\sqrt{5/3} \simeq -1.29$. As expected, best agreement is at the smallest values of Γ and D. Below $x = -1.29$, where theory predicts a discontinuity in the activation energy R, experiment shows a steep rise in R. A comparison with white-noise results for the same potential (Fig. 6) shows that the steepness is genuine. The white-noise strength was chosen to give the same curvature of $R(x)$ at $x = -1$. Note that it is not meaningful to compare QMN and white noise at the same D. The steepest-descent theory is valid for small D, i.e., D small compared to R. For QMN, the expression for R contains a large factor ω_0^2/Γ which is of course absent in the white-noise case. Thus D values which are relatively large numerically may still be small from the point of view of QMN induced fluctuations. The rounding off of the discontinuity in $R(x)$ predicted by the lowest-order theory at $\bar{x}$ can be treated by perturbation theory in Γ. This forms the subject of the next section.

IV. THEORY OF THE PROBABILITY DISTRIBUTION

A. General formulation

The quantitative theory of the shape of the tails of the quasistationary distribution about a stable state i, $p_i(x)$,

is based on the path-integral formulation [11,29,30] in conjunction with the method of optimal fluctuation [22,26,31] or steepest-descent method [6]. See Ref. [32] for a review. To logarithmic accuracy, the calculation of $p_i(x)$ reduces to the solution of the variational problem,

$$\ln(p_i(x)/p_i(x_i)) = -R_i(x)/D, \quad D = T/\Gamma(\omega_0^2 - \Gamma^2),$$

$$R_i(x) \simeq \min\left\{ \frac{1}{2} \int_{-\infty}^{\infty} dt\, f(t) F(-id/dt) f(t) \right.$$
$$\left. + \int_{-\infty}^{0} dt\, \lambda(t)(\dot{x} + U'(x) - f(t)) \right\}, \quad (35)$$

$$F(\omega) = D/\Phi(\omega).$$

The corresponding variational equations are of the form

$$F(-id/dt)f(t) = \lambda(t),$$
$$\dot{\lambda}(t) = U''(x)\lambda(t), \quad (36)$$
$$\dot{x} + U'(x) = f(t),$$

while the boundary conditions are as follows:

$$x(-\infty) = x_i, \quad f(\pm\infty) = 0, \quad \lambda(-\infty) = 0,$$
$$x(0) = x, \quad \lambda(t) = 0 \quad \text{for} \quad t > 0. \quad (37)$$

The function $R_i(x)$ in (35) is the "activation energy" for the passage to a point x from the equilibrium position x_i. We note that only the first term in the variational functional in (35) contributes to R_i; the second term has been added to allow for the interrelation (9) between $x(t)$ and $f(t)$ so as to make them independent variational variables. $\lambda(t)$ is the Lagrange multiplier.

Equations (35)–(37) provide the basis for a consistent derivation of the results of the double-adiabatic approximation considered in Sec. II, and also make it possible to go beyond this limit and consider nonadiabatic corrections. If the interrelation (10) between the characteristic decrement Γ, the relaxation time t_r, and the characteristic frequency ω_0 holds, it is convenient to seek the solution of the variational equations (36) as a superposition of fast oscillating terms and terms which are slowly varying on average:

$$f(t) = \sum_{\alpha=\pm} f_\alpha(t) \exp(i\alpha\omega_0 t) + \delta f(t),$$
$$x(t) = \sum_{\alpha=\pm} x_\alpha(t) \exp(i\alpha\omega_0 t) + x_c(t), \quad (38)$$
$$\lambda(t) = \sum_{\alpha=\pm} \lambda_\alpha(t) \exp(i\alpha\omega_0 t) + \lambda_c(t).$$

We shall choose the auxiliary variables $x_\pm, x_c, \lambda_\pm,$ $\lambda_c, f_\pm, \delta f$ in such a way that they will be nearly smooth on the optimal path (36); the fast-oscillating terms in them will be small. To describe them we shall use the three-variable potential V as introduced in (16). We define $x_\pm, \lambda_\pm$ by the relations

$$x_\alpha(t) = (i\alpha\omega_0)^{-1}f_\alpha(t), \qquad \lambda_\alpha(t) = (i\alpha\omega_0)^{-1}V_{c\alpha}''\lambda_c(t),$$

$$(39)$$

i.e., we relate the complex amplitude of the oscillations of the coordinate to the amplitude of the force, while the oscillating term in the variable λ is related to asymmetry of the potential $U(x)$.

The equations for x_c, λ_c are of the form

$$\dot{x}_c + V_c' - \delta f = \Delta_x, \qquad \dot{\lambda}_c - V_{cc}''\lambda_c = \Delta_\lambda. \qquad (40)$$

The explicit expressions for Δ_x, Δ_λ follow from (36). To zeroth order in the nonsmoothness of the auxiliary variables under consideration, Δ_x is the sum of terms proportional to $\exp(in\omega_0 t)$ with $n \neq 0$. They result in fast-oscillating corrections to x_c of order $(\omega_0 t_r)^{-1}, \Gamma/\omega_0$ that are thus small compared both with x_c and $|x_\pm|$ ($|x_c| \sim |x_\pm|$) and are neglected in what follows. The terms in Δ_λ oscillating as $\exp(in\omega_0 t)$ ($n \neq 0, \pm 1$) give rise to corrections $\sim (\lambda_c/\omega_0 t_r)\exp(in\omega_0 t)$ to $\lambda(t)$. They can be ignored because apart from being small, they are also nonresonant with $f(t)$ [$f(t)$ and $\lambda(t)$ are interrelated by Eq. (36)] and cause extremely small corrections $\sim (\Gamma^2/\omega_0^3 t_r)\lambda_c \exp(in\omega_0 t)$ to $f(t)$. The smooth term in Δ_λ is $\sim \lambda_\pm/t_r \sim \lambda_c/\omega_0 t_r^2 \ll \lambda_c V_{cc}''$ and thus can be neglected as well. The term oscillating as $\exp(\pm i\omega_0 t)$ can be easily seen to give rise to a correction that contains an extra factor $(\omega_0 t_r)^{-1}$ as compared with $\lambda_\pm$. Therefore, to lowest order in $(\omega_0 t_r)^{-1}$, we can replace (40) by the equations

$$\dot{x}_c + V_c' - \delta f = 0, \qquad (41a)$$

$$\dot{\lambda}_c - V_{cc}''\lambda_c = 0. \qquad (41b)$$

Fourier transforming (36), (6) gives

$$f(t) = \int_{-\infty}^{0} dt'\phi(t-t')\lambda(t'),$$

$$\phi(t) = \frac{1}{2}\Gamma\tilde{\omega}_0 \exp(-\Gamma|t|)$$

$$\times \left[(\tilde{\omega}_0 - i\Gamma)^{-1}\exp(-i\tilde{\omega}_0|t|) + \text{c.c.}\right], \qquad (42)$$

$$\tilde{\omega}_0 = (\omega_0^2 - \Gamma^2)^{1/2}.$$

To lowest order in Γ/ω_0, $(\omega_0 t_r)^{-1}$ one obtains from (38) and (42)

$$f_\alpha(t) = \frac{1}{2}\Gamma \int_{-\infty}^{0} dt' \exp(-\Gamma|t-t'|)\lambda_\alpha(t')$$

$$+ \frac{i\alpha\Gamma}{2\omega_0}\lambda_c(0)\exp(-\Gamma|t|) \qquad (43)$$

and

$$\delta f(t) = (4\Gamma^2/\omega_0^2)\lambda_c(t). \qquad (44)$$

It is seen from (39), (41a), (43), and (44) that the auxiliary variables introduced in Eq. (38) are indeed smooth [we note that $\lambda(t)$ and $d^4 f(t)/dt^4$ are discontinuous at $t = 0$; the value of $\lambda_c(0)$ in (43) and in what follows is that of $\lambda_c(t)$ for $t \to 0-$].

The characteristic time scale for the variation of $f_\pm(t)$ is Γ^{-1}, and the smooth part of the force $\delta f(t)$ is indeed small for not too large λ_c. If the double adiabaticity holds, the term $\delta f(t)$ can be neglected in (41) and the solution of this equation takes the form

$$x_c(t) = x_c^{(\text{ad})}(x_+(t), x_-(t)),$$

$$(45)$$

$$V_c' = V_c'(x_c^{(\text{ad})}, x_+, x_-) = 0,$$

which coincides with (18) and (19). According to (45), the center of vibrations occupies the minimum (over x_c) of the averaged potential $V(x_c, x_+, x_-)$ for given x_+, x_-. As was shown in Sec. II, the system cannot go beyond a certain point in this approximation and the distribution has a singularity there. The nonadiabatic theory is considered in the next subsection.

B. Nonadiabatic theory

It can be seen from Eqs. (41)–(43) that the value of $\lambda_c(0)$ increases sharply as x approaches the boundary point $\overline{x}$ [26]. As a consequence, the smooth component of the force $\delta f(t)$ which drives the center of vibrations x_c also increases, and should be taken into account in (41a). Moreover, relatively fast terms appear in $x_\pm(t)$. Their effect must also be considered. The theory which takes these factors into account is nonadiabatic.

The nonadiabaticity parameter is

$$\epsilon = (\Gamma/\overline{V}_{cc}'')^{1/2}, \qquad (46)$$

where $\overline{V} \equiv V(\overline{x}_c, \overline{x}_+, \overline{x}_-)$. We study the large ω_0 limit, i.e., we assume $(\omega_0 t_r)^{-1} \ll \epsilon$. As we shall see, there is a critical range where

$$|\delta f(0)|/\overline{V}_{cc}'' \sim |x_+(0) - \overline{x}_+| \sim |x_c(0) - \overline{x}_c| \sim \epsilon$$

$$\text{for } |x - \overline{x}| \sim \epsilon \quad (47)$$

Writing $x_c = x_c^{(\text{ad})} + \delta x_c$ and linearizing (41a) about the adiabatic solution gives

$$\delta\dot{x}_c + \dot{x}_c^{(\text{ad})} + \delta x_c \overline{V}_{cc}'' - \delta f = 0. \qquad (48)$$

Derivatives of V at the end point $x(0)$ will be approximated by their values at $\overline{x}$, when calculating nonadiabatic corrections.

It follows immediately from (41b) and (44) that

$$\delta f(t) = \delta f(0)\exp(\overline{V}_{cc}''t). \qquad (49)$$

Differentiating (43) and using (39), (44), (49), and the relation $\overline{V}_{cc}'' = \overline{V}_{ca}''$ gives

$$\dot{x}_\pm = \frac{1}{4}\delta f(t)$$

from which (45) yields

$$\dot{x}_c^{(\text{ad})} = -\frac{1}{2}\delta f. \qquad (50)$$

The solution of (48) is now seen to be

$$\delta x_c = \frac{3}{4} \delta f(t) / \overline{V}''_{cc}. \qquad (51)$$

One more relation is required to close the system of equations for the smooth variables. It can be obtained by first integrating (41b) and substituting (39) to give

$$\lambda_\alpha(t) = (i\alpha\omega_0)^{-1} \lambda_c(0) V''_{c\alpha}(t) \exp \int_0^t dt' \, V''_{cc}(t').$$

Expansion about $t = 0$ then gives

$$\lambda_\alpha(t) = (i\alpha\omega_0)^{-1} \lambda_c(0) \exp[V''_{c\alpha}(0)t]$$
$$\times \left(V''_{c\alpha}(0) + \Delta V''_{c\alpha}(t) + V''_{c\alpha}(0) \int_0^t dt' \Delta V''_{cc}(t') \right),$$
$$|t| \ll \Gamma^{-1} \quad (52)$$

where

$$\Delta V''_{cs}(t) = V''_{cs}(t) - V''_{cs}(0)$$

$$= \overline{V}'''_{ccs}(x_c(t) - x_c(0))$$

$$+ \sum_{\beta=\pm} \overline{V}'''_{c\beta s}(x_{-\beta}(t) - x_{-\beta}(0)) \quad (s = \pm, c). \quad (53)$$

Integration of (43) using (48)–(52) is straightforward and results in

$$f_+(0) = f_-(0)$$
$$= \frac{i\Gamma}{2\omega_0} \lambda_c(0) \left[\left(1 - \frac{V''_{c+}(0)}{V''_{cc}(0)} \right) + \frac{1}{8} \frac{\delta f(0)}{\overline{V}''^2_{cc}} \left(\overline{V}'''_{c+-} + \overline{V}'''_{c++} - \overline{V}'''_{ccc} - \overline{V}'''_{cc-} \right) \right]. \qquad (54)$$

On expanding the first bracket about the adiabatic solution and changing variables from $f_\pm$ to $x_\pm$ one obtains

$$x_+(0) = x_-(0) = \frac{1}{8} \frac{\delta f(0)}{\Gamma} \left[1 - \frac{V''^{(\mathrm{ad})}_{c+}}{V''^{(\mathrm{ad})}_{cc}} \right]$$
$$- \frac{1}{64} \frac{\delta f^2(0)}{\Gamma \overline{V}''^2_{cc}}$$
$$\times (7\overline{V}'''_{cc+} - 5\overline{V}'''_{ccc} - \overline{V}'''_{c++} - \overline{V}'''_{c+-}). \qquad (55)$$

Finally, invoking (38), the activation energy $R_i(x)$ for reaching a point x starting from the equilibrium position x_i can be written as

$$R_i(x) \simeq \frac{1}{2} \int_{-\infty}^0 dt \left[\sum_\alpha f_\alpha(t) \lambda^*_\alpha(t) \right.$$
$$+ \lambda_c(t) \sum_\alpha f_\alpha(t) \exp(i\alpha\omega_0 t)$$
$$\left. + \lambda_c(t) \delta f(t) \right]. \qquad (56)$$

Evaluation of the second and third integrals is simple. Exploiting the fact that the main terms in $f_\pm(t)$ vary much more slowly than $\lambda_\pm$ allows the first to be split into two:

$$f_\alpha(t) \lambda^*_\alpha(t) = i\alpha\omega_0 \left[x_\alpha(0) + \frac{1}{4} \int_0^t dt' \delta f(t') \right] \lambda^*_\alpha(t). \qquad (57)$$

The first term in (57) has already been integrated in (43) (ignoring contributions of order ϵ^2) while integration of the second is straightforward. Collecting contributions together gives

$$R(x) = \frac{2\omega_0^2}{\Gamma} \left(x_+^2(0) + \frac{3}{64} \frac{\delta f^2(0)}{\Gamma \overline{V}''_{cc}} \right), \qquad (58a)$$

where

$$x = 2x_+(0) + x_c^{(\mathrm{ad})}(0) + \frac{3}{4} [\delta f(0) / \overline{V}''_{cc}]. \qquad (58b)$$

Equations (55) and (58) give an analytic solution for the quasistationary probability distribution for a QMN driven system (quoted earlier, without derivation, in Ref. [15]). They were used to generate the theoretical curves plotted in Fig. 5.

Some simplification occurs for x close to $\overline{x}$. In terms of small parameters $\Delta x_\pm = x_\pm(0) - \overline{x}_\pm$, $\Delta x_c = x_c^{(\mathrm{ad})}(0) - \overline{x}_c$, one has

$$1 - \frac{V''_{c+}(0)^{(\mathrm{ad})}}{V''_{cc}(0)^{(\mathrm{ad})}} \simeq \rho \Delta x_+ \qquad (59)$$

with

$$\rho = (4\overline{V}'''_{cc+} - 2\overline{V}'''_{ccc} - \overline{V}'''_{c++} - \overline{V}'''_{c+-}) / \overline{V}''_{cc} \qquad (60)$$

and (58b) reduces to

$$x - \overline{x} = \rho (\Delta x_+)^2 + \frac{3}{4} \delta f(0) / \overline{V}''_{cc}, \qquad (61)$$

which makes it easier to follow the evolution of $R(x)$ from (55). However, we emphasize that the full equations (55) and (58) are valid for arbitrary x. Far from the singular point $\overline{x}$, the function $R_i(x)$ is smooth $(1/R_i)(dR_i/dx) \sim 1$. In this range $\delta f(0) \sim \Gamma$ and the $\delta f(0)^2$ terms can be neglected. For x close to $\overline{x}$ these terms become substantial and $R_i(x)$ becomes extremely steep: $(1/R_i)(dR_i/dx) \sim (\overline{V}''_{cc}/\Gamma)^{1/2}$ for $\rho(\overline{x} - x) \sim (\Gamma / V''_{cc})^{1/2}$. [The steep section of $R_i(x)$ lies on the side of $\overline{x}$ which

is inaccessible in the $\Gamma \to 0$ limit.] The slope of $R_i(x)$ increases with decreasing Γ, i.e., with decreasing width of the peak in the QMN power spectrum. We stress that such a steep coordinate dependence occurs in the *logarithm* of the quasistationary distribution and $p_i(x)$ itself is much steeper still.

V. MONOSTABLE POTENTIALS

QMN also gives rise to interesting effects in symmetric single-well potentials. The solution of the variational equations (39) and (40) in the adiabatic approximation gives here the same results as Eq. (25) obtained from qualitative arguments. We know that for a harmonic potential $U(x) = \frac{1}{2}a_2x^2$, the stochastic differential equations (5) and (9) are linear and the probability distribution, including the prefactor, can be obtained exactly for arbitrary a_2, Γ, ω_0. The result reads [33]

$$
p(x) = \left(\frac{A}{2\pi}\right)^{1/2} \exp\left(-\frac{1}{2}Ax^2\right),
$$

$$
A = \frac{a_2\omega_0^2}{\Gamma D(\omega_0^2 - \Gamma^2)} \frac{(a_2^2 + \omega_0^2)^2 - 4\Gamma^2 a_2^2}{a_2(a_2^2 + \omega_0^2) - 4\Gamma^2 a_2 + 2\Gamma\omega_0^2}.
$$

(62)

This probability density is shown to coincide with experiment to within 5% in Fig. 7(a) over a wide range of a_2 values. In the regime $\Gamma \ll a_2 \ll \omega_0$ Eq. (62) reduces to $p(x) \propto (-\omega_0^2 x^2/2\Gamma D)$, which is independent of the curvature of the potential. Even more remarkably, Ref. [26]
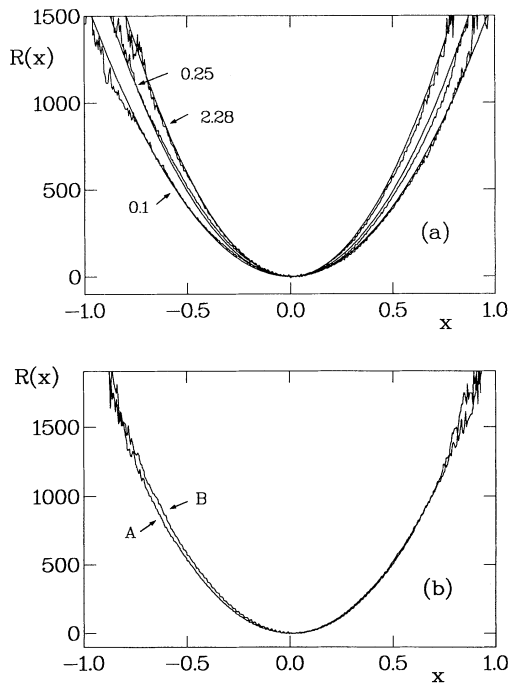

FIG. 7. (a) Quasistationary distributions for harmonic potentials $U(x) = \frac{1}{2}a_2x^2$. Pairs of curves (theory and experiment, the experiment being the jagged line) are labeled with the value of a_2. (b) Effect of including anharmonic terms: $A, U(x) = \frac{1}{2}x^2; B, U(x) = \frac{1}{2}x^2 + \frac{1}{4}x^4$.

and the arguments of Sec. II show that the latter form is unaffected by anharmonic terms $U(x) = \frac{1}{2}\sum_n a_{2n}x^{2n}$. The experimental data of Fig. 7(b) verify this prediction.

VI. CONCLUSIONS

The experimental data obtained in this paper confirm unequivocally that the dependence of the escape probabilities on the noise intensity in a system driven by QMN is of activation type. The activation energies obtained in analog and digital simulations are virtually coincident and are extremely close, within the accuracy of the experiment, to the theoretical results. An important feature is that they *exceed* the characteristic activation energy for reaching the potential barrier top from a corresponding stable state. This corresponds to the fact that crossing the PBT in the course of fluctuations does not result in a transition, with overwhelming probability, for QMN driven systems. Indeed for $\Gamma = 0.021$, $\omega_0 = 9.81$, it was observed that only one in a hundred *series* of crossings resulted in a transition (by series we mean multiple crossings of the PBT by an oscillating coordinate within one outburst of the noise).

It has been demonstrated explicitly that the steep rise in the absolute value of the *logarithm* of the probability distribution provides evidence of a singular feature of fluctuations. It is not associated with any sort of singularity of the regular motion of the system in the absence of noise, but is related instead to the interplay of fluctuations and dynamics. The theory provided in the paper fully describes this unusual behavior. The theory and experiment are in good agreement. QMN may be viewed as the prototype of a class of more complicated colored noises, whose power spectra peak at finite frequencies ω_0, instead of zero frequency. The dramatic effects revealed by this paper motivate further examination of such noise processes.

APPENDIX

The algorithm used for the numerical simulations is based on Refs. [24] and [34], and generalizes that of [24] to the case where the eigenvalues are not necessarily complex conjugate. The equations one wants to integrate are

$$
\ddot{f} = -2\Gamma\dot{f} - \omega_0^2 f + \xi(t),
$$

$$
\dot{x} = -U'(x) + f,
$$

(A1)

where ξ is a Gaussian random variable with average zero and variance $4\Gamma T$. The first step is to integrate the

stochastic evolution of the variable f, which can be done exactly (in a statistical sense), due to the linearity of the equations of motion. As shown in Ref. [34] (see also [24]), the idea is to split the motion of f into a deterministic plus a stochastic part.

From Eq. (A1) for the evolution of y it is possible to write

$$\dot{f} = v, \quad \dot{v} = -2\Gamma v - \omega_0^2 f + \xi(t). \qquad (A2)$$

Introducing $W \equiv (y, v)$, $F(t) \equiv (0, \xi(t))$, and the matrix M defined by

$$M = \begin{pmatrix} 0 & 1 \\ -\omega_0^2 & -2\Gamma \end{pmatrix},$$

one can rewrite Eq. (A2) as

$$\dot{W} = MW + F(t). \qquad (A3)$$

The formal solution of this equation is (h will be the integration time step of the numerical simulations)

$$W(t+h) = \left(\exp \int_t^{t+h} M(s)ds \right) W(t) \\ + \int_t^{t+h} \left(\exp \int_s^{t+h} M(z)dz \right) F(s)ds, \qquad (A4)$$

where the first and the second term on the right-hand side of this equation yield, respectively, the deterministic and the stochastic evolution of the vector W. It is then straightforward to derive the evolution of each component of W, although some care is necessary when the stochastic integral is evaluated. The final result can be cast in the form

$$f(t+h) = A_{11} f(t) + A_{12} v(t) + w_1,$$
$$\qquad \qquad \qquad \qquad \qquad \qquad (A5)$$
$$v(t+h) = A_{21} f(t) + A_{22} v(t) + w_2,$$

where w_1, w_2 are Gaussian stochastic variables with zero average and as yet unknown standard deviations and cross correlation.

The matrix A follows immediately from the first term in Eq. (A4). For the stochastic variables, on the other hand, one matches correlations of the w_1, w_2 in Eq. (A5) to the corresponding quantities in Eq. (A4).

The most general expression for w_1, w_2 would be of the form

$$w_1 = B_{11} z_1,$$
$$\qquad \qquad \qquad \qquad \qquad (A6)$$
$$w_2 = B_{21} z_1 + B_{22} z_2,$$

where z_1, z_2 are two uncorrelated Gaussian variables with zero average and standard deviation one. We will write explicit expressions for A_{ij} and B_{ij} below.

Now, we need to integrate the equation for $x(t)$. This is done with a first-order predictor of Adams-Bashforth

type, followed by a second-order corrector of Adams-Moulton type [35,36]. The deterministic drift $[-U'(x)]$ of Eq. (A1) poses no problem. On the other hand, the integration of the stochastic variable $y(t)$ from t to $t+h$ generates yet another stochastic variable $r(t)$ for which we write

$$r(t) = A_{31} y(t) + A_{32} v(t) + w_3 \qquad (A7)$$

and

$$w_3 = B_{31} z_1 + B_{32} z_2 + B_{33} z_3, \qquad (A8)$$

where z_3 is another Gaussian variable with zero average and standard deviation one, not correlated to z_1, z_2.

We first predict

$$x'(t+h) = x(t) + h[-U'(x(t))] + r(t+h) \qquad (A9)$$

and then correct as

$$x(t+h) = \{x'(t+h) + x(t) + h[-U'(x'(t+h))] \\ + r(t+h)\}/2. \qquad (A10)$$

Now, let us give explicit expressions for the various quantities. Introducing eigenvalues

$$\lambda_\pm \equiv -\Gamma \pm \sqrt{\Gamma^2 - \omega_0^2} \qquad (A11)$$

and

$$\Omega^2 \equiv \omega_0^2 - \Gamma^2 \qquad (A12)$$

(Ω^2 can be negative), we have for the matrix A

$$A_{11} = \frac{i}{2\Omega} \left\{ \lambda_+ e^{h\lambda_-} - \lambda_- e^{h\lambda_+} \right\},$$
$$A_{12} = \frac{i}{2\Omega} \left\{ e^{h\lambda_-} - e^{h\lambda_+} \right\},$$
$$A_{21} = -\frac{i\lambda_+ \lambda_-}{2\Omega} \left\{ e^{h\lambda_-} - e^{h\lambda_+} \right\},$$
$$\qquad \qquad \qquad \qquad \qquad \qquad (A13)$$
$$A_{22} = \frac{i}{2\Omega} \left\{ \lambda_- e^{h\lambda_-} - \lambda_+ e^{h\lambda_+} \right\},$$
$$A_{31} = \frac{i}{2\Omega} \left\{ \frac{\lambda_-}{\lambda_+} \left(e^{h\lambda_+} - 1 \right) - \frac{\lambda_+}{\lambda_-} \left(e^{h\lambda_-} - 1 \right) \right\},$$
$$A_{32} = \frac{i}{2\Omega} \left\{ \frac{e^{h\lambda_-} - 1}{\lambda_-} - \frac{e^{h\lambda_+} - 1}{\lambda_+} \right\}.$$

The matrix A turns out to be always real.

Explicit expressions for the matrix B are very cumbersome. It is simpler to write the expressions for the moments of the variables w_1, w_2, w_3 and to evaluate B numerically from the resulting equations. Suppose we knew the moments $\langle w_1^2 \rangle$, $\langle w_1 w_2 \rangle$, $\langle w_2^2 \rangle$, we have, multiplying and averaging Eq. (A5) and remembering the properties of z_1, z_2,

$$B_{11}^2 = \langle w_1^2 \rangle,$$
$$B_{12} = \langle w_1 w_2 \rangle / B_{11},$$
$$B_{22}^2 = \langle w_2^2 \rangle - B_{12}^2,$$

and similarly for w_3.

The expressions for the various moments of the variables w_1, w_2, and w_3 are

$$\langle w_1^2 \rangle = \frac{4\pi T}{2\Omega^2} \left\{ \frac{1 - e^{2h\lambda_+}}{2\lambda_+} + \frac{1 - e^{2h\lambda_-}}{2\lambda_-} - 2\frac{1 - e^{h(\lambda_+ + \lambda_-)}}{\lambda_+ + \lambda_-} \right\},$$

$$\langle w_1 w_2 \rangle = \frac{4\pi T}{2\Omega^2} \left\{ -\frac{e^{2h\lambda_+} + e^{2h\lambda_-}}{2} + e^{h(\lambda_+ + \lambda_-)} \right\},$$

$$\langle w_2^2 \rangle = \frac{4\pi T}{2\Omega^2} \left\{ -\lambda_+ \frac{1 + e^{2h\lambda_+}}{2} - \lambda_- \frac{1 + e^{2h\lambda_-}}{2} + \frac{\lambda_+^2 + \lambda_-^2 + 2\lambda_+\lambda_- e^{h(\lambda_+ + \lambda_-)}}{\lambda_+ + \lambda_-} \right\},$$

(A14)

$$\langle w_1 w_3 \rangle = \frac{4\pi T}{2\Omega^2} \left\{ \left(e^{h\lambda_+} - 1\right) \frac{1 - e^{h\lambda_+}}{2\lambda_+^2} + \left(e^{h\lambda_-} - 1\right) \frac{1 - e^{h\lambda_-}}{2\lambda_-^2} \right.$$
$$\left. - \frac{\lambda_- \left(e^{h\lambda_+} + e^{h\lambda_-} - 1 - e^{h(\lambda_+ + \lambda_-)}\right) + \lambda_+ \left(e^{h\lambda_-} + e^{h\lambda_+} - 1 - e^{h(\lambda_+ + \lambda_-)}\right)}{\lambda_+ \lambda_- (\lambda_+ + \lambda_-)} \right\},$$

$$\langle w_2 w_3 \rangle = \frac{4\pi T}{2\Omega^2} \left\{ \frac{2e^{h\lambda_+} - 1 - e^{2h\lambda_+}}{2\lambda_+} + \frac{2e^{h\lambda_-} - 1 - e^{2h\lambda_-}}{2\lambda_-} \right.$$
$$\left. + \frac{2 - e^{h\lambda_+} - e^{h\lambda_-} + \frac{\lambda_+}{\lambda_-} \left(e^{h\lambda_-} - 1\right) e^{h\lambda_+} + \frac{\lambda_-}{\lambda_+} \left(e^{h\lambda_+} - 1\right) e^{h\lambda_-}}{\lambda_+ + \lambda_-} \right\},$$

$$\langle w_3^2 \rangle = \frac{4\pi T}{\Omega^2} \left\{ \frac{4e^{h\lambda_+} - 3 - 2h\lambda_+ - e^{2h\lambda_+}}{4\lambda_+^3} + \frac{4e^{h\lambda_-} - 3 - 2h\lambda_- - e^{2h\lambda_-}}{4\lambda_-^3} \right.$$
$$\left. + \frac{h\lambda_+\lambda_- + \frac{\lambda_+ \lambda_-}{\lambda_+ + \lambda_-} \left(e^{2h(\lambda_+ + \lambda_-)} - 1\right) - \lambda_- \left(e^{h\lambda_+} - 1\right) - \lambda_+ \left(e^{h\lambda_-} - 1\right)}{(\lambda_+ + \lambda_-)^2} \right\},$$

which allows us to derive the necessary elements of the matrix B and hence the coefficients for the numerical algorithm. Note that all moments are real.

---

* Present address: Department of Engineering, University of Warwick, Coventry, CV4 7AL, United Kindgom.

[1] A. Einstein, Ann. Phys. (Leipzig) 17, 549 (1905).

[2] M. von Smoluchowski, Ann. Phys. (Leipzig) 21, 756 (1906).

[3] For reviews see K. Lindenberg, B. J. West, and G. P. Tsironis, Rev. Solid State Sci. 3, 143 (1990); H. R. Brand, C. R. Doering and R. E. Ecke, J. Stat. Phys. 54, 1111 (1989), and references therein; K. Lindenberg, B. J. West, and J. Masoliver, in *Noise in Nonlinear Dynamical Systems*, edited by F. Moss and P. V. E. McClintock (Cambridge University Press, Cambridge, 1989), Vol. 1, p. 110; P. Grigolini, *ibid.*, p. 161.

[4] R. F. Fox, Phys. Rev. A 37, 911 (1988).

[5] J. F. Luciani and A. D. Verga, Europhys. Lett. 4, 255 (1987); J. Stat. Phys. 50, 567 (1988).

[6] A. J. Bray and A. J. McKane, Phys. Rev. Lett. 62, 493 (1989); A. J. McKane, H. C. Luckock, and A. J. Bray, Phys. Rev. A 41, 644 (1990).

[7] A. J. McKane, Phys. Rev. A 40, 4050 (1989).

[8] A. J. Bray, A. J. McKane, and T. J. Newman, Phys. Rev. A 41, 657 (1990).

[9] H. C. Luckock and A. J. McKane, Phys. Rev. A 42, 1982 (1990).

[10] K. M. Rattray and A. J. McKane, J. Phys. A 24, 1215

(1991); 24, 4375 (1991).

[11] L. Pesquera, M. A. Rodriguez, and E. Santos, Phys. Lett. 94A, 287 (1983); P. Colet, H. S. Wio, and M. San Miguel, Phys. Rev. A 39, 6094 (1989); H. S. Wio, P. Colet, M. San Miguel, L. Pesquera, and M. A. Rodriguez, *ibid.* 40, 7312 (1989).

[12] M. M. Klosek-Dygas, B. J. Matkowsky, and Z. Schuss, SIAM J. Appl. Math. 48, 425 (1988); J. Stat. Phys. 54, 1309 (1989).

[13] Hu Gang and H. Haken, Phys. Rev. A 41, 7078 (1990).

[14] The various theories were compared with the results of digital simulations in R. Mannella, V. Palleschi, and P. Grigolini, Phys. Rev. A 42, 5946 (1990).

[15] M. I. Dykman, P. V. E. McClintock, N. D. Stein, and N. G. Stocks, Phys. Rev. Lett. 67, 933 (1991).

[16] W. H. Louisell, *Radiation and Noise in Quantum Electronics* (McGraw-Hill, New York, 1964).

[17] M. Lax, in *Statistical Physics, Phase Transitions and Superconductivity*, edited by N. Chretien, E. P. Grass, and S. Deser (Gordon and Breach, New York, 1968).

[18] See A. S. Barker, Jr. and A. J. Sievers, Rev. Mod. Phys. Suppl. No. 2 47, S1 (1975).

[19] *Proceedings of the International Conference on Defects in Insulating Crystals, Parma, 1988* (University of Parma, Parma, 1988).

[20] K. K. Rebane, *Impurity Spectra of Solids: Elementary Theory of Vibrational Structure* (Plenum, New York, 1970).

[21] A. A. Maradudin, in *Solid State Physics*, edited by F. Seitz and D. Turnbull (Academic, New York, 1966), Vol. 19, p. 2.

[22] M. I. Dykman and M. A. Krivoglaz, in *Soviet Physics Reviews*, edited by I. M. Khalatnikov (Harwood Academic, New York, 1984), Vol. 5, p. 265.

[23] W. Ebeling and L. Schimansky-Geier, in *Noise in Nonlinear Dynamical Systems* (Ref. [3]), p. 279.

[24] L. Schimansky-Geier and Ch. Zülicke, Z. Phys. B **79**, 451 (1990).

[25] A. Igarashi and T. Munakata, J. Phys. Soc. Jpn. **57**, 2439 (1988).

[26] M. I. Dykman, Phys. Rev. A **42**, 2020 (1990).

[27] H. A. Kramers, Physica (Utrecht) **7**, 284 (1940).

[28] P. V. E. McClintock and F. Moss, in *Noise in Nonlinear Dynamical Systems* (Ref. [3]), Vol. 3, p. 243.

[29] R. P. Feynman and A. R. Hibbs, *Quantum Mechanics and Path Integrals* (McGraw-Hill, New York, 1965).

[30] R. Phythian, J. Phys. A **10**, 777 (1977).

[31] M. I. Dykman and M. A. Krivoglaz, Zh. Eksp. Teor. Fiz. **77**, 60 (1979) [Sov. Phys.—JETP **50**, 30 (1979)].

[32] M. I. Dykman and K. Lindenberg, in *Some Problems in Statistical Physics*, edited by G. H. Weiss (SIAM, Philadelphia, in press).

[33] This equation was misprinted in [15].

[34] R. Mannella and V. Palleschi, Phys. Rev. A **40**, 3381 (1989).

[35] See L. Lapidus and J. H. Seinfeld, *Numerical Solution of Ordinary Differential Equations* (Academic, New York, 1971) for details in the deterministic case, and E. K. Blum, *Numerical Analysis and Computational Theory and Practice* (Wiley, New York, 1972).

[36] W. Rümelin, SIAM J. Numer. Anal. **19**, 604 (1982).